Revealing metabolic flexibility of *Candidatus* Accumulibacter phosphatis through redox cofactor analysis and metabolic network modeling

Running title: Metabolic flexibility of Accumulibacter

Leonor Guedes da Silva#, Karel Olavarria Gamez, Joana Castro Gomes, Kasper Akkermans, Laurens Welles, Ben Abbas, Mark C.M. van Loosdrecht, Sebastian Aljoscha Wahl

Department of Biotechnology, Delft University of Technology, The Netherlands

#Address correspondence to Leonor Guedes da Silva, LeonorGuedesdaSilva@gmail.com

These investigations were supported by the SIAM Gravitation Grant 024.002.002, the Netherlands Organization for Scientific Research (NWO). The authors declare no conflict of interest.

KEYWORDS

Candidatus Accumulibacter phosphatis, Polyphosphate Accumulating Organisms (PAO), Enhanced Biological Phosphate Removal (EBPR), Central carbon metabolism, Redox cofactors, Flux Balance Analysis, Enzymatic assays

ABSTRACT

Environmental fluctuations in the availability of nutrients lead to intricate metabolic strategies. *Candidatus* Accumulibacter phosphatis, a polyphosphate accumulating organism (PAO) responsible for enhanced biological phosphorus removal (EBPR) from wastewater treatment systems, is prevalent in aerobic/anaerobic environments. While the overall metabolic traits of these bacteria are well described, the inexistence of isolates has led to controversial conclusions on the metabolic pathways used.

Here, we experimentally determined the redox cofactor preference of different oxidoreductases in the central carbon metabolism of a highly enriched *Ca.* A. phosphatis culture. Remarkably, we observed that the acetoacetyl-CoA reductase engaged in polyhydroxyalkanoates (PHA) synthesis is NADH-preferring instead of the generally assumed NADPH dependency. Based on previously published meta-omics data and the results of enzymatic assays, a reduced central carbon metabolic network was constructed and used for simulating different metabolic operating modes. In particular, scenarios with different acetate-to-glycogen consumption ratios were simulated. For a high ratio (i.e. more acetate), a polyphosphate-based metabolism arises as optimal with a metabolic flux through the glyoxylate shunt. In case of a low acetate-to-glycogen ratio, glycolysis is used in combination with reductive branch of the TCA cycle. Thus, optimal metabolic flux strategies will depend on the environment (acetate uptake) and on intracellular storage compounds availability (polyphosphate/glycogen).

This metabolic flexibility is enabled by the NADH-driven PHA synthesis. It allows for maintaining metabolic activity under varying environmental substrate

48 conditions, with high carbon conservation and lower energetic costs compared
49 to NADPH dependent PHA synthesis. Such (flexible) metabolic redox coupling
50 can explain PAOs' competitiveness under oxygen-fluctuating environments.

51 IMPORTANCE

52 Here we demonstrate how microbial metabolism can adjust to a wide range
53 of environmental conditions. Such flexibility generates a selective advantage
54 under fluctuating environmental conditions. It can also explain the different
55 observations reported in PAO literature, including the capacity of *Ca.*
56 Accumulibacter phosphatis to act like glycogen accumulating organisms
57 (GAO). These observations stem from slightly different experimental conditions
58 and controversy only arises when one assumes metabolism can only operate
59 in one single mode. Furthermore, we also show how the study of metabolic
60 strategies is possible when combining -omics data with functional assays and
61 modeling. Genomic information can only provide the potential of a
62 microorganism. The environmental context and other complementary
63 approaches are still needed to study and predict the functional application of
64 such metabolic potential.

INTRODUCTION

Natural habitats of microorganisms are dynamic environments with intermittent supply of nutrients. Under these dynamic conditions, organisms are selected that can accumulate growth substrates when these are abundant to compensate for periods when these are exhausted (1).

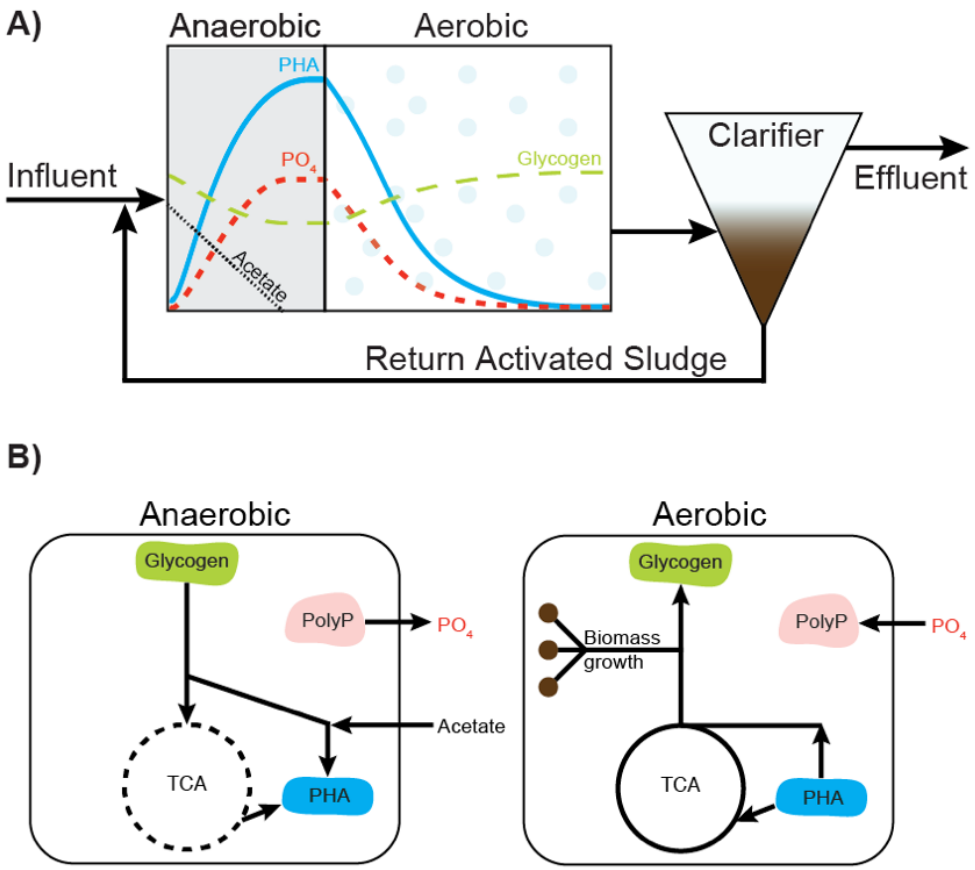

Figure 1 – Schematic diagram of an EBPR process with nutrient/polymer profiles (A) and corresponding metabolic strategy (B). Recirculated activated sludge containing PAOs is mixed with influent wastewater in an anaerobic reactor. To compensate for the absence of an external electron acceptor, Accumulibacter use their polyphosphate and glycogen reserves to take up organic carbon sources (e.g. acetate) and accumulate them in the form of polyhydroxyalkanoates (PHA). Phosphate is released at this stage. The TCA cycle is represented by a dashed line has it can have different operating modes. When oxygen becomes available, Accumulibacter makes use of their PHA storage to grow, to replenish glycogen and polyphosphate. The re-accumulation of polyphosphate in growing biomass and subsequent purge of this biomass leads to the net removal of phosphate from wastewater. Adapted from (2, 3). PHA, polyhydroxyalkanoates; PolyP, polyphosphate; PO_4, phosphate; TCA, tricarboxylic acid cycle.

83 Enhanced biological phosphate removal (EBPR) from wastewater is
84 designed to make use of such physiological feature by circulating activated
85 sludge through alternating zones with or without an external electron acceptor
86 here respectively defined as aerobic/anaerobic (see Figure 1A) (4, 5). This
87 environment selects for polyphosphate accumulating organisms (PAOs) like
88 *Candidatus* Accumulibacter phosphatis (hereafter referred to as
89 Accumulibacter). These bacteria thrive under these dynamic conditions thanks
90 to a complex metabolic strategy encompassing the cycling of three common
91 storage polymers: polyphosphate, glycogen and polyhydroxyalkanoates (PHA).
92 Of these, polyphosphate stands out for allowing for fast and competitive
93 harvesting of organic matter in the absence of an external electron acceptor
94 (see Figure 1B).

95 In the past decades, a number of researchers have derived hypotheses
96 about Accumulibacter's (anaerobic) physiology (4, 6–8). One of the most
97 important inconclusive discussions is the source of reducing power for the
98 anaerobic accumulation of polyhydroxyalkanoates (PHA) from volatile fatty
99 acids (e.g. acetate, propionate), as reviewed by Zhou *et al* (9). Most
100 experimental approaches were adequate to study the general physiology of
101 Accumulibacter species, however the inherent population heterogeneity has
102 not yet been sufficiently addressed; for example, only recently researchers
103 have reported different Accumulibacter clades showing different kinetic
104 characteristics leading to different metabolic operations (10). Furthermore,
105 novel meta-omics approaches were used, which allowed for Accumulibacter-
106 targeted (culture-independent) analysis without the interference of other, non-
107 Accumulibacter, sub-populations. A comprehensive overview of the
108 physiological studies published on Accumulibacter can be found in the

109 Supplementary Document S1. In one of the metatranscriptomic studies (11),
110 Oyserman and colleagues highlighted the need for validating assumptions
111 often made in metabolic models of Accumulibacter. In particular, they refined
112 the discussion on reducing power sources and requirements by making a
113 distinction between the different redox cofactors, NADH and NADPH. This
114 distinction imposes a constraint between sources and sinks for each redox
115 cofactor, which can only be alleviated by energy-consuming
116 transhydrogenase(-like) mechanisms or using electrons for hydrogen
117 production. However, in their analysis, the specificity of the involved
118 oxidoreductases was derived from analogy with other organisms.

119 In Accumulibacter, reducing power is required for the conversion of acetate
120 to 3-hydroxybutyrate (3HB), the monomer of the reserve polymer poly-3-
121 hydroxybutyrate (PHB). The intermediate reduction step is catalyzed by the
122 enzyme acetoacetyl-CoA reductase (AAR). In PHA accumulating bacteria such
123 as *Cupriavidus necator* and *Zoogloea ramigera*, the preferred electron donor
124 cofactor of the AAR is NADPH (12), which was the cofactor assumed by
125 analogy for Accumulibacter (11). However, AARs accepting both NADH and
126 NADPH have been reported for *Azotobacter beijerinckii* (13, 14) and
127 *Allochromatium vinosum* (15). A brief thermodynamic feasibility analysis of the
128 coupling between glycolysis and either NADPH- or NADH-preferring AAR is
129 present in the Supplementary Document S2.

130 So far and to our knowledge, the nature of the cofactor accepted by
131 Accumulibacter's acetoacetyl-CoA reductase has not yet been experimentally
132 established. In this study, we addressed this knowledge gap by measuring the
133 NADH- and NADPH-dependent acetoacetyl-CoA reductase activities in a cell
134 free extract from a highly enriched culture of Accumulibacter. We further

135 extended the analysis to other key oxidoreductases involved in the anaerobic
136 metabolism of Accumulibacter. These results were then used to update
137 Accumulibacter's biochemical model and as constraints in a flux balance
138 analysis (FBA) framework. Our simulations show how the use of different
139 pathways and storage compounds lead to metabolic flexibility. Without this
140 flexibility, Accumulibacter's metabolism would become very restrictive and,
141 under unpredictable anaerobic environments, it could lead to situations were
142 only a limited fraction of the available substrate could be consumed.

143 ## MATERIALS AND METHODS

144 ### Reactor operation

145 Two independent Accumulibacter enrichments were obtained in sequencing
146 batch reactors (SBR). The main operational conditions are described in Table
147 2 and were adapted from the SBR-S as described in Welles *et al* (10).

148 ### Cell free extracts preparation

149 Broth samples (10 mL) collected from the bioreactor during both anaerobic
150 and aerobic phases were centrifuged (2500g, 10 min, 4ºC) and the pellet was
151 washed using 10 mL buffer (hereafter named Buffer 1X) containing 50 mM Tris
152 at pH 8, 5 mM $MgCl_2$, 5 mM NaCl and 5% (v/v) glycerol, and the obtained
153 suspension was centrifuged again (2500g, 10 min, 4ºC). After centrifugation,
154 pellets were kept at -20ºC for no longer than four days until further analysis. For
155 the enzymatic assay, cellular pellets were suspended in 10 mL of Buffer 1X
156 supplemented with 2 mM (L+D) 1,4-Dithiothreitol (DTT) and cOmplete™ mini
157 protease inhibitor cocktail (Roche). To avoid overheating and protein
158 denaturation, cells were kept on ice while being sonicated until the cell
159 suspension was homogenized (i.e. no granules visible). The resulting
160 suspension was centrifuged (15000g for at least 45 min, 4ºC). The obtained
161 supernatant, a cell free extract (CFE), was used for the enzymatic assays.

162 ### Enzymatic assays

163 The reaction mixtures used for each enzymatic assay are described in Table
164 1. Activities were calculated using the initial rate of reduction of $NAD(P)^+$ or
165 oxidation of NAD(P)H, which was obtained by following the changes in the
166 absorbance at 340 nm, at 30ºC. To control the contribution of putative
167 background reactions, reaction mixtures were monitored that contained all the

168 components except one substrate or without addition of CFE (see “Controls” in
169 Supplementary Document S4). The measured rates were normalized to the
170 total protein concentration in the respective CFE. The protein concentration was
171 measured using the Bradford dye-binding protein assay (Bio-Rad), using
172 known concentrations of bovine serum albumin as external standards.

173 Table 1 – Origin of the cell free extract (CFE), buffer, substrates, controls and references
174 (16–24) used for each enzymatic assay. Controls used can be found in Supplementary
175 Document S4.

CFE	Tested enzyme	Buffer	Substrates	Reference
SBR-1	acetoacetyl-CoA reductase (AAR)	1X, supplemented	200 µM acetoacetyl-CoA, 200 µM NADH or 200 µM NADPH	(16)
SBR-2	acetoacetyl-CoA reductase (AAR)	1X, supplemented	40 µM acetoacetyl-CoA, 100 µM NADH or 200 µM NADPH	(17)
SBR-2	3-hydroxybutyryl-CoA dehydrogenase (3HBDH)	1X, supplemented	100 µM 3-hydroxybutyryl-CoA 1000 µM $NAD(P)^+$	(17)
SBR-1	glucose-6-phosphate dehydrogenase (G6PDH)	1X, supplemented	2 mM glucose-6-phosphate; 2000 µM NAD^+ or 200 µM $NADP^+$	(18)
SBR-2	glucose-6-phosphate dehydrogenase (G6PDH)	1X, supplemented	4 mM glucose-6-phosphate; 400 µM $NAD(P)^+$	
SBR-2	isocitrate dehydrogenase (ICDH)	1X, supplemented	400 µM $NAD(P)^+$ 400 µM isocitrate	(19)
	malate dehydrogenase (MDH)	1X, supplemented	200 µM NAD(P)H 200 µM oxaloacetate	(20)
	malic enzyme (ME)	1X, supplemented	200 µM NADP 200 µM L-malate	(21)
	isocitrate lyase (ICL)	40 mM HEPES, pH 7, 6 mM $MgCl_2$	4 mM isocitrate, 280 µM NADH 45 units lactate dehydrogenase from rabbit muscle (Roche)	(22)
	fumarate reductase (FR)	50 mM HEPES, pH 7	15 mM fumarate 250 µM NADH	(23)
	α-ketoglutarate dehydrogenase (AKGDH)	50 mM HEPES, pH 7, 1mM $MgCl_2$, 1mM Thiamine pyrophosphate, 2.5 mM DTT	2 mM α-ketoglutaric acid 100 µM Coenzyme A 2.5 mM $NAD(P)^+$	(24)

176

177 **Microbial community characterization**

178 The microbial community present in our enrichments has been characterized
179 by three orthogonal approaches as described below and the detailed results
180 can be found in Supplementary Document S3.

181 Fluorescence *in situ* hybridization (FISH) was used to qualitatively assess
182 the presence of Accumulibacter in the enrichment cultures. All bacteria were
183 targeted by the EUB338 mix (general bacteria probe) (25–27). Accumulibacter
184 clade I and II were targeted by the probes Acc-1-444 and Acc-2-444 (28),
185 respectively. Hybridized samples were examined with a Zeiss Axioplan-2
186 epifluorescence microscope.

187 To further confirm the specific Accumulibacter clade, the presence of the
188 gene encoding for the polyphosphate kinase I (*ppk1*) present in Accumulibacter
189 was tested as described in (29, 30) using the primers ACCppk1-254F and
190 ACCppk1-1376R targeting the *ppk1* gene from Accumulibacter-like bacteria
191 (31). The *ppk1* gene sequences obtained in this study have been deposited in
192 the GenBank database under accession numbers MH899084-MH899086.

193 To identify putative side-populations, 16S-rRNA gene amplicon sequencing
194 was applied. DNA samples from cell pellets were extracted using the DNeasy
195 UltraClean Microbial Kit (Qiagen, The Netherlands). Approximately 250 mg wet
196 biomass was treated according to the standard protocol except an alternative
197 lysis was implemented. This included a combination of 5 min of heat (65°C)
198 followed by 5 min of bead-beating for cell disruption on a Mini-Beadbeater-24
199 (Biospec, U.S.A.). After extraction the DNA was checked for quality by gel
200 electrophoresis and quantified using a Qubit 4 (Thermo Fisher Scientific,
201 U.S.A.).

202 After quality control, samples were sent to Novogene Ltd. (Hongkong, China)
203 for amplicon sequencing of the V3-4 region of the 16S-rRNA gene (position
204 341-806) on an Illumina paired-end platform. After sequencing, the raw reads
205 were quality filtered, chimeric sequences were removed and OTUs were
206 generated on the base of ≥ 97% identity. Subsequently, microbial community
207 analysis was performed by Novogene using Mothur & Qiime software(V1.7.0)
208 (32, 33). For phylogenetical determination, the most recent SSURef database
209 from SILVA (34) was used. The microbial communities in each enrichment were
210 compared based on the 10 most abundant OTUs with a distinctive genus (i.e.
211 with most reads assigned to it). The 16S-rRNA gene amplicon data have been
212 deposited in GenBank under Bioproject PRJNA490689.

213 **Anaerobic biochemical model of Accumulibacter**

214 The metabolic network shown in Figure 2 is based on the ancestral genome
215 reconstruction of Accumulibacter proposed by (2) as well as experimental
216 observations obtained here. Additionally, an extensive literature overview
217 supporting this biochemical model of Accumulibacter can be found in
218 Supplementary Document S1.

219 **Flux balance analysis (stoichiometric modeling)**

220 To estimate the possible metabolic flux distributions Flux Balance Analysis
221 (FBA) has been applied (35). The flux distribution can be obtained by
222 optimization:

223
$$v_{opt} = \arg\min_{\boldsymbol{v}} v_{CO2_{prod}} \quad \text{subject to} \begin{cases} Nv = 0 \\ v_{irr} \geq 0 \\ v_{Glyc_{deg}} = 1 - f \\ v_{Ac_{upt}} = f \end{cases}$$

224
$$\text{with } f = 0 \ldots 1 \frac{Cmol}{Cmol\ C_{consumed}}$$

225 where N is the stoichiometry matrix containing the reactions later shown in
226 Table 3 and v is the vector containing all reaction fluxes (see also
227 Supplementary Document S6). The simulation assumes that none of the
228 balanced intermediates is accumulating inside the cell (steady-state
229 assumption). This is acceptable given the long simulation period compared to
230 the turnover time of these intermediates. Inequality constraints were introduced
231 for physiologically irreversible fluxes (i.e. these should always be positive). The
232 consumption of acetate and glycogen is varied between only acetate ($f = 1$) to
233 only glycogen ($f = 0$). The respective experimental data is normalized to a
234 summed consumption of 1 Cmol (see Supplementary Document S5).

235 Commonly, maximization of biomass synthesis is used in FBA as an
236 optimization objective. However, Accumulibacter only grows aerobically and on
237 the intracellular carbon reserves (PHAs) accumulated during substrate uptake
238 in the anaerobic period. Biomass synthesis was thus assumed proportional to
239 the carbon stored as PHA. Consequently, maximal carbon conservation in
240 PHA, resp. minimal CO_2 production, is set as the cellular objective for the
241 anaerobic phase.

242 To prevent adding a stoichiometric constraint due to an assumption on the
243 proportion of the different PHA polymers possible, i.e. poly-3-hydroxybutyrate
244 (PHB), poly-3-hydroxyvalerate (PHV), poly-3-hydroxy-2-methylbutyrate
245 (PH2MB), or poly-3-hydroxy-2-methylvalerate (PH2MV), the respective
246 monomer amount is introduced, i.e. the reduced precursors Ac-CoA* and Pr-
247 CoA* such that:

248 2 Ac-CoA* → 3HB;

249 Ac-CoA* + Pr-CoA* → 3HV (or 3H2MB);

250 2 Pr-CoA* → 3H2MV;

251 **Compilation and normalization of stoichiometric data**

252 The results of the aforementioned simulations were compared to
253 stoichiometric data reported in literature for several different Accumulibacter
254 enrichments. Anaerobic-feast yields were used when available, otherwise the
255 yields of the whole anaerobic phase were used. In case of missing compound
256 rates (usually CO_2, PH2MV), these were estimated using electron and carbon
257 balancing (see Supplementary Document S5). For datasets with redundant
258 measurements, a data reconciliation method was applied (36). For all
259 calculations, we assumed acetate and glycogen monomers were the only
260 substrates and CO_2, PHB, PHV and PH2MV were the only products. In case
261 yields were reported without the respective error, the error was calculated using
262 error propagation. Here, the relative errors were assumed as follows: 5% for
263 acetate and PHB measurements, and 10% for PHV, PH2MV and glycogen
264 measurements. From the (reconciled) rates for PHB, PHV and PH2MV, the
265 respective Ac-CoA* and Pr-CoA* rates were determined and normalized to the
266 amount of consumed substrates, in Cmol.

267 # RESULTS

268 ## Characterization of Accumulibacter enrichments

269 This study was carried out using two independent Accumulibacter
270 enrichment cultures. SBR-1 contained the highest enrichment of
271 Accumulibacter observed in our lab. However, this cultivation was operating
272 close to a critical dilution rate which, unfortunately, resulted in washout (i.e.
273 enrichment deterioration) after sampling. In SBR-2, conditions were adjusted to
274 reduce the risk of washout, i.e. higher COD load and higher SRT were used.

275 Table 2 – Process parameters and key performance indicators of the two independent
276 enrichments of Accumulibacter.

	SBR-1	**SBR-2**	
pH	7.6	7.6	
T	20ºC	20ºC	
Carbon source	210 mg COD/L (63:37 Acetate:Propionate)	400 mg COD/L (75:25 Acetate:Propionate)	
Phosphate load per C	0.1 Pmol/Cmol	0.1 Pmol/Cmol	
Cycle time	6 h Settling – 76 min; Anaerobic – 135 min; Aerobic – 135 min.	6 h Settling – 30 min; Anaerobic – 112 min; Aerobic – 200 min.	
HRT	12 h	12 h	
SRT	4 days	5.6 days	
Aerobic SRT	1.5 days	3.1 days	
Anaerobic P-release per C-fed	0.58 Pmol/Cmol	~0.75 Pmol/Cmol	
Anaerobic-feast length	~41 min	~42 min	
FISH	PAO Acc I	PAO Acc I	
16S rRNA gene amplicon sequencing (dominant OTUs)	Ca_Accumulibacter Rhodopseudomonas Blastochloris	Start: Dechloromonas Ca_Accumulibacter genus from f__Hyphomonadaceae	End: Ca_Accumulibacter Chryseobacterium genus from o__Sphingobacteriales
***ppk1* analysis**	Dominant: clade IC	Dominant: clade IA	

277

278

279 For both cultures, anaerobic P-release per C-fed indicated that the PAO
280 present in the sludge are likely saturated with polyphosphate and that glycogen
281 accumulating organisms (GAO) are not present (37). Furthermore, microbial
282 characterization by FISH showed Accumulibacter from clade I were the majority
283 of the microorganisms across all biomass samples as it can be seen by the high
284 overlap between the Accumulibacter-specific probe and the general Bacteria
285 probe (micrographs available in Supplementary Document S3). The *ppk1* gene
286 analysis further specified which subclade was dominant and the 16S-rRNA
287 gene analysis provided information on the genus of the most abundant sub-
288 populations next to Accumulibacter (see Table 2 and Supplementary Document
289 S3).

290 **Redox cofactor preferences of key oxidoreductases**

291 For the simulation and interpretation of the metabolic network function it was
292 essential to identify the cofactor specificity of relevant reactions. Enzymatic
293 assays were performed using cell free extracts. While these assays cannot
294 discriminate which organism has the respective activity, the performed assays
295 still answer: 1) if an activity is not observed for the whole community, it is also
296 not present in Accumulibacter, 2) if the cell extract shows a clear preference for
297 NAD(H) or NADP(H) this is most probably also the preferred cofactor of
298 Accumulibacter which is highly enriched in the culture.

299 The enzymatic activity assay results display a clear preference which is
300 sufficient to annotate a specific cofactor. These are shown in blue in the
301 metabolic network in Figure 2. Further details can be found in Supplementary
302 Document S4. The different assay results will be presented from the sinks
303 (PHA) to the putative sources of reducing power:

304 (1) Redox cofactor preference (NADH or NADPH) of the PHA synthesis. The
305 CFE from SBR-1 had a NADH preferring acetoacetyl-CoA reductase. The
306 activity was 10x higher with NADH compared to NADPH as substrate. To
307 further confirm this cofactor preference, the acetoacetyl-CoA reductase
308 activity was assayed using CFEs from a second enrichment (SBR-2) and
309 both directions of the reaction were monitored (i.e. NAD(P)H + acetoacetyl-
310 CoA ↔ $NAD(P)^+$ + 3-hydroxybutyryl-CoA).
311 (2) Stoichiometry of glycolysis – Embden-Meyerhof-Parnas (EMP) or Entner-
312 Doudoroff (ED)? To discriminate between these pathways, the presence of
313 the glucose-6-phosphate dehydrogenase, the enzyme that catalyzes the
314 first step of ED was measured. This reaction is also common to the oxidative
315 branch of the pentose phosphate pathway (oxPP). No activity was found in
316 the CFEs from both SBRs. The biological positive control, a CFE from *P.*
317 *putida* KT2440, showed activity with both NAD^+ and $NADP^+$, as expected
318 (38). Therefore, Accumulibacter nor the community have an active ED or
319 oxPP pathway leaving EMP as glycolytic route.
320 (3) Alternative NADPH sources. For many organisms oxPP is an important
321 source of NADPH for growth (20). This activity was not found in
322 Accumulibacter, raising the question if NADPH could be provided by other
323 reaction like isocitrate dehydrogenase. The oxidation of isocitrate was
324 tested using either NAD^+ or $NADP^+$. The activity with $NADP^+$ was more than
325 70x higher, indicating that isocitrate dehydrogenase is a relevant source of
326 NADPH in Accumulibacter.
327 Additionally, the activity of other oxidoreductases and anaplerotic routes
328 was measured: i) the reduction of oxaloacetate to malate (catalyzed by
329 malate dehydrogenase) had, at least, 55x higher activity when using NADH

than NADPH. Because of the small activity observed when using NADPH, it was not possible to independently study the cofactor preference of the malic enzyme (oxidation of malate to pyruvate); ii) the glyoxylate shunt was also found to be active and to have an activity comparable to the positive biological control *E. coli* grown in acetate (well known to make use of the glyoxylate shunt (39)); and lastly, iii) fumarate reductase and α-ketoglutarate dehydrogenase were also tested but their activities were very low compared to all other enzymes tested in our study.

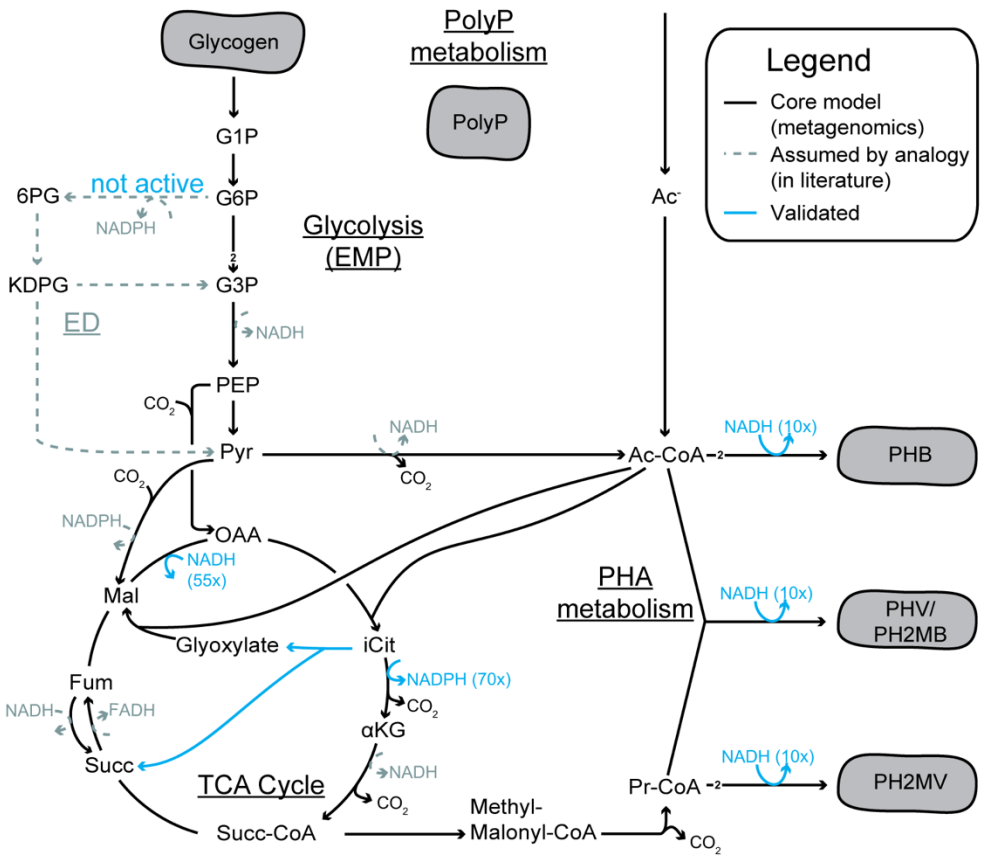

Figure 2 – Central carbon metabolic network of Accumulibacter including redox cofactor preference of oxidoreductases assayed in this study. A simplified version of this network (Table 3) was used for the simulations. The values shown corresponds to the factor difference between the preferred cofactor and the alternative one. This metabolic network is based on the ancestral genome reconstruction done by (2). The arrows show the expected flux direction under anaerobic conditions. The untested cofactor preferences (in gray) remain as assumed by analogy with other microorganisms. Despite not being annotated in the genome, the ED pathway has been suggested as the route for glycogen degradation (40, 41). A more extensive

347 overview of evidence for each pathway can be found in Supplementary Document S1. G1P,
348 glucose-1-phosphate; G6P, glucose-6-phosphate; 6PG, 6-phosphogluconate; KDPG, 2-keto-
349 3-deoxy-6-phosphogluconate; G3P, glyceraldehyde-3-phosphate; PEP, phosphoenolpyruvate;
350 Pyr, pyruvate; OAA, oxaloacetate; Ac-CoA, Acetyl-CoA; iCit, isocitrate; αKG, α-ketoglutarate;
351 Succ-CoA, succinyl-CoA; Succ, succinate; Fum, fumarate; Mal, malate; Pr-CoA, propionyl-
352 CoA; Ac^-, acetate; EMP, Embden-Meyerhof-Parnas; TCA, tricarboxylic acid cycle.

353 **Anaerobic stoichiometric model construction**

354 Based on the defined reaction network (Figure 2 and Table 3) the balance of
355 reducing equivalents by Accumulibacter during anaerobic acetate conversion
356 to PHAs was studied quantitatively. Note that the network from Figure 2 was
357 further simplified (Table 3) based on the presented evidence that PHA
358 accumulation in Accumulibacter is NADH-consuming rather than previously
359 assumed NADPH preference based on genome annotations. The cofactor
360 NADH can be regenerated from other electron carriers like NADPH or
361 ferredoxin using transhydrogenases without any energetic cost for the cell (20).

362 This is not the case for FADH, which would require an input of energy (ATP)
363 to be re-oxidized using NAD^+. Currently, there is still no experimentally
364 validated mechanism on how Accumulibacter could re-oxidize FADH in the
365 absence of an external electron acceptor (e.g. oxygen or nitrate). Therefore, for
366 this simulation, we blocked this FADH producing step in the TCA cycle (i.e.
367 Succ-CoA to Fum) and for the remaining reactions we neglected the different
368 types of redox cofactors by simply balancing “electrons” (note that each redox
369 cofactor carries 2 electrons and, in some publications, these are simply referred
370 to as [H]). Since the FADH producing step in the TCA cycle is blocked, only the
371 oxidative branch (OAA to Succ-CoA via ICDH and AKGDH) and/or the
372 reductive branch (OAA to Succ-CoA via MDH and FR) are possible.

373

374 Table 3 – Stoichiometry used for flux balance analysis (in mol basis) to simulate
375 Accumulibacter's anaerobic metabolism. Reversible reaction: ↔, irreversible reaction: →. Note
376 that these are lumped reactions, and each may involve several enzymatic steps. A
377 comprehensive overview of the physiological studies published on Accumulibacter supporting
378 this stoichiometric model can be found in the Supplementary Document S1.

Pathway	Stoichiometry	Enzyme assayed in this study
Glycolysis (EMP)	$(Glycogen)_1 \rightarrow 2$ Pyr + 4 electrons	G6PDH
Pyruvate to Acetyl-CoA	Pyr → Ac-CoA + 2 electrons + CO_2	
Pyruvate to Oxaloacetate	Pyr + CO_2 ↔ OAA	
Oxidative TCA branch	OAA + Ac-CoA → Succ-CoA + 2 CO_2 + 4 electrons	ICDH AKGDH
Reductive TCA branch (reverse TCA)	OAA + 4 electrons → Succ-CoA	MDH FR
Glyoxylate shunt	2 Ac-CoA → Succ-CoA + 2 electrons	ICL
Succinate-propionate shunt	Succ-CoA ↔ Pr-CoA + CO_2	
Ac-CoA* production (precursor for 3HB, 3HV and 3HMB)	Ac-CoA + electron → Ac-CoA* (* means "+1electron")	AcAc-CoA red
Pr-CoA* production (precursor for 3H2MV, 3HV and 3HMB)	Pr-CoA + electron → Pr-CoA* (* means "+1electron")	AcAc-CoA red

379

380 In contrast to electron balances, the ATP balance cannot be used as there
381 are still too many unknowns: 1) how much ATP can be generated from efflux of
382 ions (potassium, magnesium and phosphate) associated with polyphosphate
383 hydrolysis; 2) how much ATP is required for acetate uptake; 3) how much is

384 needed to upgrade redox cofactors (i.e. transfer electrons from low to high
385 potential cofactors); 4) and how much ATP is used for cellular maintenance.
386 Therefore, ATP is not balanced in this simulation. Nevertheless, it is important
387 to note that the different pathways used for redox balancing will lead to different
388 levels of ATP generation. Thus, in cases of polyphosphate limitation, the
389 metabolism could prefer pathways with higher ATP-yield.

390 Experiments show that the ratio between glycogen and acetate consumption
391 by PAOs is variable, e.g. between high/low temperature (42) or
392 polyphosphate/glycogen availability (37, 43, 44). To reflect this variability,
393 simulations were performed for a range of acetate and glycogen mixtures
394 ranging from only acetate to only glycogen and results were compared to
395 experimental data reported in literature.

396 For the anaerobic sequestration of acetate as PHA, acetate needs to be
397 reduced (Ac-CoA*). The Ac-CoA* optimum in Figure 3 corresponds to the
398 situation in which most carbon is kept inside the cell. The required reducing
399 power can come from either glycolysis (glycogen breakdown) or glyoxylate
400 shunt (acetate oxidation) operation. The different modes are presented in
401 Figure 4. These modes respectively form the extreme left and right values of
402 the optimum line in Figure 3. If glycogen degradation can supply exactly the
403 amount of electrons needed for the uptake and conversion of acetate, then only
404 Ac-CoA* (as PHB) is produced and there is no need to use any part of the TCA
405 cycle (Figure 4B, and highest PHB yield in Figure 3).

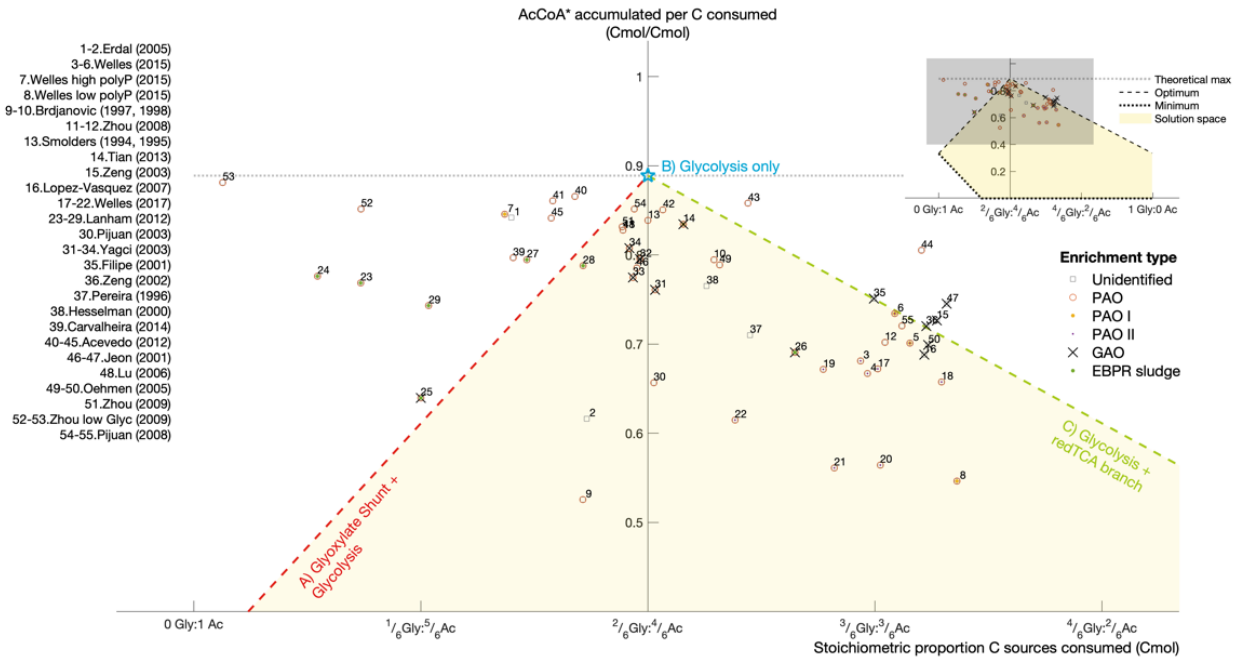

Figure 3 – The amount of Ac-CoA* accumulated (PHB and PHV precursor) depends on the different proportion of glycogen to acetate consumed and on the available pathways. The three optimum redox balancing strategies are shown in Figure 4 ABC. From 0 to approx. 2/6 glycogen Cmol, it can be considered that bacteria are performing a polyphosphate-based metabolism (PAM, optimum line in red) and from approx. 3/6 to 1 glycogen Cmol, a glycogen-based metabolism (GAM, optimum line in green) is used. The “optimum” and “minimum” lines were obtained by minimizing and maximizing CO_2 production, respectively. The feasible solution space (in yellow) lies in between these two cellular objectives, in which a mixture of different redox balancing strategies is used. The minimum carbon conserving strategy is the one that only uses the oxidative TCA branch. Experimental datasets were retrieved from (10, 37, 50–59, 41, 42, 44–49) and normalized to respect carbon and energy conservation principles (see Supplementary Document S5). Similar plots for Pr-CoA*, CO_2, alternative simulations and including error bars on the experimental data points can be found in Supplementary Document S6.

415 The optimum can probably only be achieved with polyphosphate as ATP
416 source. In a typical GAO-like metabolism, an excess of glycogen is degraded
417 compared to the acetate consumed to supply all ATP needed. This leads to the
418 generation of an excess of reducing power, which is used to produce Pr-CoA*
419 leading to PHAs more reduced than PHB (e.g. PHV or PH2MV), using the
420 reductive TCA branch (Figure 4C). On the other hand, in a PAO-like metabolism
421 the amount of reducing equivalents generated by glycolysis is usually lower
422 than required to reduce all consumed acetate. In this situation, part of the
423 acetate is oxidized to produce reducing equivalents. Such oxidation is possible
424 via an active glyoxylate shunt which was also found from the enzymatic assays.
425 The simulations show this as the optimal pathway to produce PHAs when
426 glycogen is limiting (Figure 4A), i.e. it allows for higher carbon conservation (i.e.
427 higher PHA yield) than the “horseshoe” TCA operation.

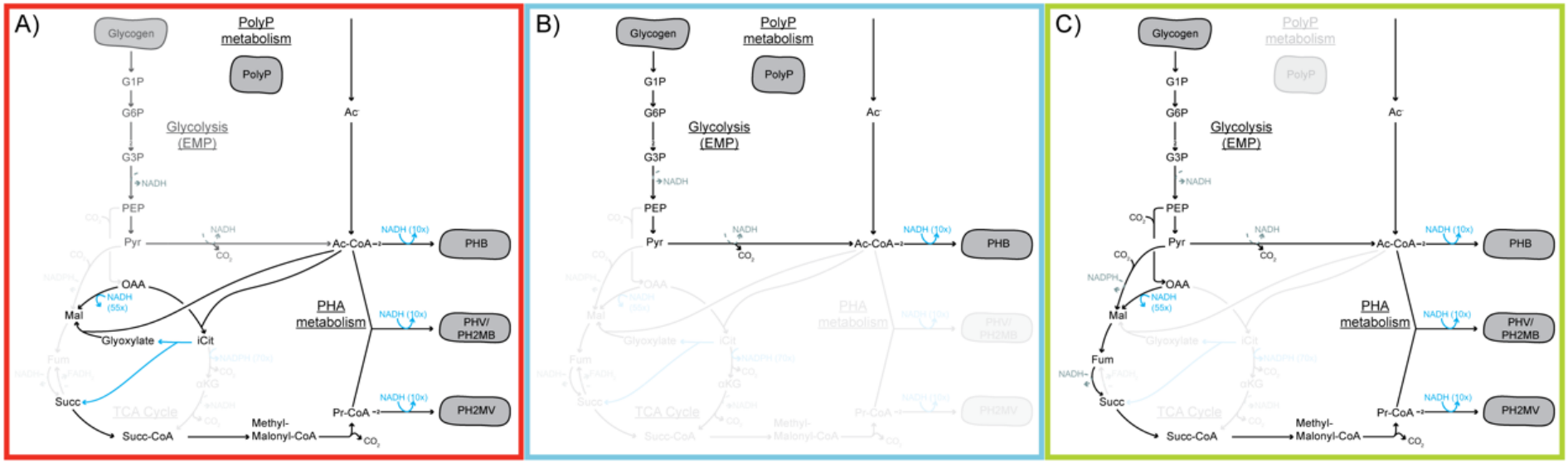

Figure 4 – Different optimum redox balancing strategies for Accumulibacter under anaerobic conditions. A) When little glycogen is degraded and is not enough to reduce all acetate to PHB, the glyoxylate shunt as recommended by (55) is the most optimal way to provide these electrons. B) When the stoichiometric amount of glycogen is degraded for acetate reduction to PHB, there is no real need to operate any part of the TCA cycle to balance redox and only PHB is then produced, as proposed in (60). C) When more glycogen than needed for acetate reduction is degraded, the reductive TCA branch can be used as proposed by (55) for GAOs to sink electrons in more reduced PHAs (e.g. PHV and PH2MV).

434 # DISCUSSION

435 ## Characterization of Accumulibacter enrichments

436 The discussion will be based on the observed high PAO enrichment of mainly
437 *Ca.* Accumulibacter phosphatis clade I. Consequently, extrapolations of these
438 results to Accumulibacter clade II or GAOs are speculative until further
439 validation using respective environments for enrichments (10, 47, 61–64).

440 ## Updated biochemical (stoichiometric) model

441 The presented study shows that the metabolic traits of Accumulibacter
442 enable a flexible metabolic operation under anaerobic conditions. This flexibility
443 is made possible by their energy and reducing power storage, enabling the
444 observed phenotypes: fast anaerobic acetate uptake and anaerobic PHB
445 synthesis (decoupled from growth). The flexible reducing power balancing by
446 Accumulibacter depends on the nature of the redox cofactors used – here,
447 enzymatic assays were performed to define the redox cofactor preferences of
448 the main oxidoreductases in the central metabolic pathways of Accumulibacter.

449 The key finding from these assays is the NADH-preferring PHA accumulation
450 in Accumulibacter. This NADH-preference allows for a direct consumption of
451 the NADH produced in most of Accumulibacter's reducing power sources. This
452 also eliminates the need for NADH into NADPH conversion, which was
453 suggested earlier by (11) using the membrane-bound transhydrogenase
454 (PntAB) driven by proton motive force. Although there are previous reports
455 showing NADH-driven PHB accumulation (13, 65–68), the level of NADH
456 preference of the acetoacetyl-CoA reductase from Accumulibacter is striking.
457 Further characterization of this enzyme was undertaken by Olavarria and

458 colleagues (in preparation). This observation allows to re-think the role of PHAs:
459 we hypothesize that depending on the environment where microorganisms
460 thrive, PHA accumulation will play a role as carbon reservoir during metabolic
461 over-flow (NADPH-driven accumulation) or as an electron reservoir during
462 scarcity of external electron acceptors (NADH-driven accumulation). Thus, for
463 Accumulibacter, PHA is essentially a fermentation product.

464 A related finding was the absence of activity of the first step of the
465 sometimes-implicated ED glycolytic pathway. These results match those
466 observed by (42) and in (69) for GAOs, where no $NADP^+$ dependent glucose-
467 6-phosphate dehydrogenase activity was found. The experimental findings are
468 in line with the absence of key ED genes in the genome annotations of
469 Accumulibacter and closest relatives *Dechloromonas aromatica* and *Azoarcus*
470 *sp. EbN1* (64, 70). Furthermore, no enzymatic activity of the ED pathway with
471 NAD^+ as electron acceptor (38) was observed.

472 These findings are in contradiction with earlier ^{13}C NMR studies (40, 41),
473 which indicated that the ED pathway was more likely the route for glycolysis
474 than EMP. Nevertheless, it has to be noted that these early studies comprise
475 interpretations of ^{13}C patterns using simplified metabolic models, with limited
476 information on the reversibility of each reaction and potentially with reactions
477 missing; these are common pitfalls of the ^{13}C-labelling method (71). Also note
478 that these ^{13}C NMR studies were performed before the first draft genome of
479 Accumulibacter was available (70), and only the ^{13}C pattern in the different
480 PHAs was measured and not in the metabolic intermediates of each pathway
481 used.

482 While NADPH is not required anaerobically by Accumulibacter, this reducing
483 cofactor has to be produced aerobically to drive biomass synthesis. Here,
484 isocitrate dehydrogenase was found $NADP^+$ dependent. This is consistent with
485 the observation that most acetate consumers will use this conversion to
486 produce NADPH for their anabolism (72) and confirms the protein annotation
487 found in (64). Since PHA accumulation is now known to be NADH-preferring
488 and without another sink of NADPH, the latter might accumulate anaerobically
489 and thereby inhibit the isocitrate dehydrogenase reaction. Alternatively, a
490 soluble transhydrogenase could convert this NADPH into NADH and allow the
491 oxidative branch of the TCA to be operational under anaerobic conditions.

492 Regarding the activity of other TCA oxidoreductases and anaplerotic routes:
493 i) the oxidation of malate using NAD^+ was also found in the studies of (42); ii)
494 the glyoxylate shunt was also found active as observed in assays done by (41,
495 42, 73) and metatranscriptomics/proteomics studies by (2, 63, 74–76), which is
496 expected as this is the anaplerotic route that allows for microorganisms to
497 convert C2 sources like acetate into C4 building blocks for anabolism (72); and
498 iii) fumarate reductase and α-ketoglutarate dehydrogenase activities were very
499 low compared to all other enzymes tested in our study and alike in the studies
500 of (42). An α-ketoglutarate:ferredoxin oxidoreductase has been identified in
501 Accumulibacter's genome and proteome (64). This has not been assayed here
502 as sufficient evidence was collected suggesting an anaerobic operation mode
503 via the glyoxylate shunt rather than a full or partial oxidative TCA cycle.

504

505

506 **Flexible anaerobic metabolism – Adjustments depending on the**
507 **environment and intracellular storage compounds**

508 As (9) suggested in their review, the flexibility of Accumulibacter's
509 metabolism is likely the major reason why there is controversy in literature
510 regarding how reducing power is balanced under anaerobic conditions. Long-
511 term exposure to set conditions (e.g. pH, temperature, oxidation level of the
512 substrate, nutrient availability, counter-ions, SRT, settling time) will select for
513 the best strategy for those conditions, but short-term perturbations of those set
514 conditions have shown that Accumulibacter seems to still be able to solve the
515 redox balancing problem even if sub-optimally regarding carbon conservation
516 (10, 43, 44, 77). Thus, based on our analysis, we observe that there is not one
517 fixed stoichiometry, but a range of possible stoichiometries that in the end are
518 defined by the relative proportions of each of the intervening substrates,
519 supplied to the system or produced by a side-population (e.g. acetate,
520 glycogen, polyphosphate, other VFAs, oxygen, nitrate, hydrogen).

521 The simulations showed Accumulibacter can operate in three distinct modes
522 (and combinations in between): A) when reducing equivalents from glycolysis
523 are limiting compared to the acetate imported (Yagci's model (55)); B) when
524 glycolysis supplies exactly enough reducing equivalents to convert all imported
525 acetate into PHB (Mino's model (60)); and lastly C) when glycolysis is producing
526 an excess of reducing equivalents (alike Yagci's model for GAOs (55)).

527 The anaerobic use of the glyoxylate shunt in a PAO-like metabolism to
528 provide for the reducing equivalents needed for PHA accumulation is supported
529 by the studies of (55, 73); However, as seen in Figure 3, it does not explain the
530 higher levels of Ac-CoA* found (points above the red optimum line) when a shift

531 to more reduced PHAs (Pr-CoA*) was expected. This indicates that there might
532 be an alternative process that allows the cell to conserve extra carbon, in other
533 words, accumulate more Ac-CoA* and less Pr-CoA*. It could be that 1) fully
534 anaerobic conditions were not attained when performing the experiments, or
535 that 2) another side population is providing electrons in the form of a more
536 reduced organic substrate or even hydrogen gas (78) or 3) Accumulibacter has
537 yet another, alternative way of balancing redox which has yet to be described
538 and demonstrated.

539 Also for the scenario where glycolysis produces an excess of reduced
540 cofactors as in a GAO-like metabolism, a few experimental data points fall
541 outside the feasible solution space (points above the green optimum line in
542 Figure 3); these could be explained in the case that Accumulibacter produces
543 H_2 to solve an excess of NADH as described by (11).

544 **The multilayered complexity of a physiological analysis of**
545 **Accumulibacter**

546 The experimental data gathered are likely also influenced by the intrinsic
547 heterogeneity of Accumulibacter enrichments; clade differences, population
548 heterogeneity or even different environment (e.g. depending on the position of
549 the cell in a floc/granule). Therefore, experimental data points under the
550 optimum line in Figure 3 likely represent mixtures of cells, each with a different
551 metabolic mode (Figure 4 A, B or C). Furthermore, any kinetic limitation (i.e.
552 pathway capacity) may also explain a sub-optimal, mixed phenotype.

553 Additionally, if all enzymatic machinery is available, it seems possible that
554 the same cell might change modes depending on the environment and its
555 intracellular storage dynamics. Particularly, availability of acetate (e.g.

556 transition feast/famine) and/or polyphosphate storage as well as glycogen can
557 trigger shifts in metabolic mode.

558 Despite the heterogeneity and noise, the experimental data outside the
559 solution space suggests this stoichiometric model is still incomplete to
560 represent all experimental conditions. The solution space expands for example
561 when (1) allowing for hydrogen production in excess glycogen-to-acetate
562 conditions or (2) the oxidation of acetate in a fully operational TCA cycle in a
563 glycolysis-limiting scenario. With these reactions, all experimental data can be
564 explained (see Supplementary Document S6). The first is supported by the
565 detection of hydrogen gas produced by an Accumulibacter enrichment (11). For
566 the latter, a full TCA cycle has been previously suggested based on ^{13}C NMR
567 observations (58) and stoichiometric analyses by (43). Additionally, a novel
568 protein has been proposed based on metagenomic analysis that could allow for
569 full TCA operation under anaerobic conditions (70); however, there is still no
570 direct biochemical experimental evidence that indeed validates a full anaerobic
571 TCA operation. Some indirect observation is presented in (79). Here, labelled
572 propionate was used as substrate and ^{13}C enrichment was found in the PHV
573 fragments that come from acetyl-CoA. This labeling pattern can be explained
574 by a full TCA, but this is not the only metabolic route that could explain this
575 observation.

576 Alternatively, it should also be considered that, alike many (strict) anaerobes,
577 Accumulibacter may use electron bifurcation mechanisms (80) via ferredoxin
578 oxidoreductases to allow for alternative pathways in the central carbon
579 metabolism.

580 **CONCLUSION**

581 In this study a network-based modeling approach was used to unravel the
582 metabolic flexibility of Accumulibacter under dynamic conditions. The approach
583 integrates findings and hypotheses derived from previous meta-omics studies
584 as well as different physiological datasets and biochemical assays.

585 The developed metabolic model demonstrates the flexibility in metabolic
586 function and could explain previous controversy in PAO literature. The NADH
587 dependent PHA synthesis is both an efficient link to catabolic pathways as well
588 as key for enabling metabolic flexibility. Depending on the exact history and
589 cultivation conditions, Accumulibacter can exhibit different metabolic
590 phenotypes; the metabolic network can handle different combinations of carbon
591 sources (i.e. acetate and glycogen) adjusting the use of glycolysis (EMP),
592 different branches of the TCA cycle (incl. glyoxylate shunt) and potentially other
593 pathways not yet considered. This poses a challenge to predictive EBPR
594 modeling, as this implies that stoichiometry is not fixed, but variable, spanning
595 continuously from polyphosphate to glycogen-based phenotypes.

596 This metabolic versatility is likely what allows Accumulibacter to be, in most
597 situations, very close to a carbon conservation optimum, which is key to ensure
598 their competitiveness in the dynamic environments of EBPR systems.

ACKNOWLEDGEMENTS

These investigations were supported by the SIAM Gravitation Grant 024.002.002, the Netherlands Organization for Scientific Research (NWO). The authors would like to thank Roel van de Wijgaart, Alexandre Carnet, Hein van der Wall, Koen Verhagen, David Weissbrodt, Alex Salazar, and Thomas Abeel for their collaboration in this project. The authors would also like to thank to Sergio Tomás Martínez and Eleni Vasilakou for proofreading and Ben Oyserman for his invaluable advice on this manuscript.

COMPETING INTERESTS

The authors declare no conflict of interest.

609 **REFERENCES**

610 1. Van Loosdrecht MCM, Pot M a., Heijnen JJ. 1997. Importance of bacterial storage
611 polymers in bioprocesses. Water Sci Technol 35:41–47.

612 2. Oyserman BO, Moya F, Lawson CE, Garcia AL, Vogt M, Heffernen M, Noguera DR,
613 McMahon KD. 2016. Ancestral genome reconstruction identifies the evolutionary
614 basis for trait acquisition in polyphosphate accumulating bacteria. ISME J 10:2931–
615 2945.

616 3. McMahon KD, Read EK. 2013. Microbial contributions to phosphorus cycling in
617 eutrophic lakes and wastewater. Annu Rev Microbiol 67:199–219.

618 4. Seviour RJ, Mino T, Onuki M. 2003. The microbiology of biological phosphorus
619 removal in activated sludge systems. FEMS Microbiol Rev 27:99–127.

620 5. Barnard JL. 1976. A review of Biological Phosphorous Removal in the Activated
621 Sludge Process. Water Sa 2:136–144.

622 6. Seviour RJ, McIlroy S. 2008. The microbiology of phosphorus removal in activated
623 sludge processes-the current state of play. J Microbiol 46:115–124.

624 7. Mino T, van Loosdrecht MCM, Heijnen JJ. 1998. Microbiology and biochemistry of
625 the enhanced biological phosphate removal process. Water Res 32:3193–3207.

626 8. Oehmen A, Lemos PC, Carvalho G, Yuan Z, Keller J, Blackall LL, Reis M a M. 2007.
627 Advances in enhanced biological phosphorus removal: From micro to macro scale.
628 Water Res 41:2271–2300.

629 9. Zhou Y, Pijuan M, Oehmen A, Yuan Z. 2010. The source of reducing power in the
630 anaerobic metabolism of polyphosphate accumulating organisms (PAOs) - A mini-
631 review. Water Sci Technol 61:1653–1662.

632 10. Welles L, Tian WD, Saad S, Abbas B, Lopez-Vazquez CM, Hooijmans CM, van
633 Loosdrecht MCM, Brdjanovic D. 2015. Accumulibacter clades Type I and II
634 performing kinetically different glycogen-accumulating organisms metabolisms for
635 anaerobic substrate uptake. Water Res 83:354–366.

636 11. Oyserman BO, Noguera DR, del Rio TG, Tringe SG, McMahon KD. 2016.
637 Metatranscriptomic insights on gene expression and regulatory controls in
638 Candidatus Accumulibacter phosphatis. ISME J 10:810–22.

639 12. Madison LL, Huisman GW. 1999. Metabolic Engineering of Poly (3-
640 Hydroxyalkanoates): From DNA to Plastic. Microbiol Mol Biol Rev 63:21–53.

641 13. Ritchie GAF, Senior PJ, Dawes EA. 1971. The Purification and Characterization of
642 Acetoacetyl-Coenzyme A Reductase from Azotobacter beijerinckii. Biochem J
643 121:309–316.

644 14. Senior PJ, Beech GA, Ritchie GA, Dawes EA. 1972. The role of oxygen limitation
645 in the formation of poly- -hydroxybutyrate during batch and continuous culture of
646 Azotobacter beijerinckii. Biochem J 128:1193–201.

647 15. Liebergesell M, Steinbüchel A. 1992. Cloning and nucleotide sequences of genes
648 relevant for biosynthesis of poly(3-hydroxybutyric acid) in Chromatium vinosum
649 strain D. Eur J Biochem 209:135–50.

650 16. Satoh Y, Tajima K, Tannai H, Munekata M. 2003. Enzyme-catalyzed poly(3-
651 hydroxybutyrate) synthesis from acetate with CoA recycling and NADPH
652 regeneration in Vitro. J Biosci Bioeng 95:335–341.

653 17. Chohan, Copeland. 1998. Acetoacetyl coenzyme A reductase and
654 polyhydroxybutyrate synthesis in rhizobium (Cicer) sp. Strain CC 1192. Appl
655 Environ Microbiol 64:2859–63.

656 18. Olavarria K, Marone MP, da Costa Oliveira H, Roncallo JC, da Costa Vasconcelos
657 FN, da Silva LF, Gomez JGC. 2015. Quantifying NAD(P)H production in the upper

658 Entner-Doudoroff pathway from Pseudomonas putida KT2440. FEBS Open Bio
659 5:908–15.

660 19. Dean AM, Golding GB. 1997. Protein engineering reveals ancient adaptive
661 replacements in isocitrate dehydrogenase. Proc Natl Acad Sci U S A 94:3104–9.

662 20. Fuhrer T, Sauer U. 2009. Different biochemical mechanisms ensure network-wide
663 balancing of reducing equivalents in microbial metabolism. J Bacteriol 191:2112–
664 2121.

665 21. Bologna FP, Andreo CS, Drincovich MF. 2007. Escherichia coli malic enzymes: two
666 isoforms with substantial differences in kinetic properties, metabolic regulation, and
667 structure. J Bacteriol 189:5937–46.

668 22. Giachetti E, Pinzauti G, Vanni P. 1984. A new continuous optical assay for isocitrate
669 lyase. Experientia 40:227–228.

670 23. Hillier AJ, Jericho RE, Green SM, Jago GR. 1979. Properties and function of
671 fumarate reductase (NADH) in Streptococcus lactis. Aust J Biol Sci 32:625–35.

672 24. Bunik VI, Denton TT, Xu H, Thompson CM, Cooper AJL, Gibson GE. 2005.
673 Phosphonate Analogues of α-Ketoglutarate Inhibit the Activity of the α-Ketoglutarate
674 Dehydrogenase Complex Isolated from Brain and in Cultured Cells †. Biochemistry
675 44:10552–10561.

676 25. Daims H, Brühl A, Amann R, Schleifer KH, Wagner M. 1999. The domain-specific
677 probe EUB338 is insufficient for the detection of all Bacteria: development and
678 evaluation of a more comprehensive probe set. Syst Appl Microbiol 22:434–44.

679 26. Amann RI. 1995. In situ identification of micro-organisms by whole cell hybridization
680 with rRNA-targeted nucleic acid probes, p. 331–345. *In* Akkermans, ADL, Van
681 Elsas, JD, De Bruijn, FJ (eds.), Molecular Microbial Ecology Manual. Springer
682 Netherlands, Dordrecht.

683 27. Amann RI, Binder BJ, Olson RJ, Chisholm SW, Devereux R, Stahl DA. 1990.
684 Combination of 16S rRNA-targeted oligonucleotide probes with flow cytometry for
685 analyzing mixed microbial populations. Appl Environ Microbiol 56:1919–25.

686 28. Flowers JJ, He S, Yilmaz S, Noguera DR, McMahon KD. 2009. Denitrification
687 capabilities of two biological phosphorus removal sludges dominated by different
688 "Candidatus Accumulibacter" clades. Environ Microbiol Rep 1:583–588.

689 29. Rubio-Rincón FJ, Welles L, Lopez-Vazquez CM, Nierychlo M, Abbas B, Geleijnse
690 M, Nielsen PH, van Loosdrecht MCM, Brdjanovic D. 2017. Long-term effects of
691 sulphide on the enhanced biological removal of phosphorus: The symbiotic role of
692 Thiothrix caldifontis. Water Res 116:53–64.

693 30. Saad SA, Welles L, Abbas B, Lopez-Vazquez CM, van Loosdrecht MCM,
694 Brdjanovic D. 2016. Denitrification of nitrate and nitrite by 'Candidatus
695 Accumulibacter phosphatis' clade IC. Water Res 105:97–109.

696 31. McMahon KD, Yilmaz S, He S, Gall DL, Jenkins D, Keasling JD. 2007.
697 Polyphosphate kinase genes from full-scale activated sludge plants. Appl Microbiol
698 Biotechnol 77:167–173.

699 32. Schloss PD, Westcott SL, Ryabin T, Hall JR, Hartmann M, Hollister EB, Lesniewski
700 RA, Oakley BB, Parks DH, Robinson CJ, Sahl JW, Stres B, Thallinger GG, Horn DJ
701 Van, Weber CF. 2009. Introducing mothur: Open-Source, Platform-Independent,
702 Community-Supported Software for Describing and Comparing Microbial
703 Communities. Appl Environ Microbiol 75:7537–7541.

704 33. Caporaso JG, Kuczynski J, Stombaugh J, Bittinger K, Bushman FD, Costello EK,
705 Fierer N, Peña AG, Goodrich JK, Gordon JI, Huttley G a, Kelley ST, Knights D,
706 Koenig JE, Ley RE, Lozupone C a, McDonald D, Muegge BD, Pirrung M, Reeder J,
707 Sevinsky JR, Turnbaugh PJ, Walters W a, Widmann J, Yatsunenko T, Zaneveld J,
708 Knight R. 2010. QIIME allows analysis of high-throughput community sequencing

709 data. Nat Methods 7:335–6.

710 34. Quast C, Pruesse E, Yilmaz P, Gerken J, Schweer T, Yarza P, Peplies J, Glöckner
711 FO. 2013. The SILVA ribosomal RNA gene database project: improved data
712 processing and web-based tools. Nucleic Acids Res 41:D590-6.

713 35. Orth JD, Thiele I, Palsson BØ. 2010. What is flux balance analysis? Nat Biotechnol
714 28:245–8.

715 36. van der Heijden RTJM, Heijnen JJ, Hellinga C, Romein B, Luyben KCAM. 1994.
716 Linear constraint relations in biochemical reaction systems: I. Classification of the
717 calculability and the balanceability of conversion rates. Biotechnol Bioeng 43:3–10.

718 37. Welles L, Abbas B, Sorokin DY, Lopez-Vazquez CM, Hooijmans CM, van
719 Loosdrecht MCM, Brdjanovic D. 2017. Metabolic response of "candidatus
720 accumulibacter phosphatis" clade II C to changes in influent P/C ratio. Front
721 Microbiol 7.

722 38. Olavarría K, Valdés D, Cabrera R. 2012. The cofactor preference of glucose-6-
723 phosphate dehydrogenase from Escherichia coli--modeling the physiological
724 production of reduced cofactors. FEBS J 279:2296–309.

725 39. Gottschalk G. 1986. Bacterial Metabolism. Springer New York, New York, NY.

726 40. Maurer M, Gujer W, Hany R, Bachmann S. 1997. Intracellular carbon flow in
727 phosphorus accumulating organisms from activated sludge systems. Water Res
728 31:907–917.

729 41. Hesselmann RPX, Von Rummell R, Resnick SM, Hany R, Zehnder a. JB. 2000.
730 Anaerobic metabolism of bacteria performing enhanced biological phosphate
731 removal. Water Res 34:3487–3494.

732 42. Erdal ZK, Erdal UG, Randall CW. 2005. Biochemistry of enhanced biological
733 phosphorus removal and anaerobic COD stabilization. Water Sci Technol 52:557–
734 567.

735 43. Zhou Y, Pijuan M, Zeng RJ, Yuan Z. 2009. Involvement of the TCA cycle in the
736 anaerobic metabolism of polyphosphate accumulating organisms (PAOs). Water
737 Res 43:1330–1340.

738 44. Zhou Y, Pijuan M, Zeng RJ, Lu H, Yuan Z. 2008. Could polyphosphate-
739 accumulating organisms (PAOs) be glycogen-accumulating organisms (GAOs)?
740 Water Res 42:2361–2368.

741 45. Brdjanovic D, Loosdrecht MCM van, Hooijmans CM, Alaerts GJ, Heijnen JJ. 1997.
742 Temperature Effects on Physiology of Biological Phosphorus Removal. J Environ
743 Eng 123:144–153.

744 46. Brdjanovic D, Van Loosdrecht MCM, Hooijmans CM, Mino T, Alaerts GJ, Heijnen
745 JJ. 1998. Effect of polyphospbate limitation on the anaerobic metabolism of
746 phosphorus-accumulating microorganisms. Appl Microbiol Biotechnol 50:273–276.

747 47. Acevedo B, Oehmen A, Carvalho G, Seco a., Borrás L, Barat R. 2012. Metabolic
748 shift of polyphosphate-accumulating organisms with different levels of
749 polyphosphate storage. Water Res 46:1889–1900.

750 48. Smolders GJF, van der Meij J, van Loosdrecht MCM, Heijnen JJ. 1994.
751 Stoichiometric model of the aerobic metabolism of the biological phosphorus
752 removal process. Biotechnol Bioeng 44:837–848.

753 49. Smolders GJF, Klop JM, van Loosdrecht MCM, Heijnen JJ. 1995. A metabolic
754 model of the biological phosphorus removal process: I. Effect of the sludge retention
755 time. Biotechnol Bioeng 48:222–233.

756 50. Tian W-D, Lopez-Vazquez CM, Li W-G, Brdjanovic D, van Loosdrecht MCM. 2013.
757 Occurrence of PAOI in a low temperature EBPR system. Chemosphere 92:1314–
758 20.

51. Zeng RJ, Yuan Z, Keller J. 2003. Model-based analysis of anaerobic acetate uptake by a mixed culture of polyphosphate-accumulating and glycogen-accumulating organisms. Biotechnol Bioeng 83:293–302.

52. López-Vázquez CM, Hooijmans CM, Brdjanovic D, Gijzen HJ, van Loosdrecht MCM. 2007. A practical method for quantification of phosphorus- and glycogen-accumulating organism populations in activated sludge systems. Water Environ Res 79:2487–2498.

53. Lanham AB. 2012. Full-scale biological phosphorus removal: quantification of storage polymers, microbial performance and metabolic modelling. Universidade Nova de Lisboa.

54. Pijuan M, Saunders AM, Guisasola A, Baeza JA, Casas C, Blackall LL. 2004. Enhanced biological phosphorus removal in a sequencing batch reactor using propionate as the sole carbon source. Biotechnol Bioeng 85:56–67.

55. Yagci N, Artan N, Çokgör EU, Randall CW, Orhon D. 2003. Metabolic model for acetate uptake by a mixed culture of phosphate- and glycogen-accumulating organisms under anaerobic conditions. Biotechnol Bioeng 84:359–373.

56. Filipe CDM, Daigger GT, Grady CPL. 2001. A metabolic model for acetate uptake under anaerobic conditions by glycogen accumulating organisms: Stoichiometry, kinetics, and the effect of pH. Biotechnol Bioeng 76:17–31.

57. Zeng R, Yuan Z, van Loosdrecht MCM, Keller J. 2002. Proposed modifications to metabolic model for glycogen-accumulating organisms under anaerobic conditions. Biotechnol Bioeng 80:277–279.

58. Pereira H, Lemos PC, Reis MAM, Crespo JPSG, Carrondo MJT, Santos H. 1996. Model for carbon metabolism in biological phosphorus removal processes based on in vivo 13C-NMR labelling experiments. Water Res 30:2128–2138.

59. Carvalheira M. 2014. The effect of key process operational conditions on enhanced biological phosphorus removal from wastewater. Universidade Nova de Lisboa.

60. Mino T, Tsuzuki Y, Matsuo T. 1987. Effect of phosphorus accumulation on acetate metabolism in the biological phosphorus removal process, p. 27–38. *In* Ramadori, R (ed.), Biological phosphate removal from wastewaters: proceedings from the International Conference of Advanced Water Pollution Control (IAWPRC). Pergamon Press, Oxford, England.

61. Flowers JJ, He S, Malfatti S, del Rio TG, Tringe SG, Hugenholtz P, McMahon KD. 2013. Comparative genomics of two “Candidatus Accumulibacter” clades performing biological phosphorus removal. ISME J 7:2301–14.

62. Welles L, Lopez-Vazquez CM, Hooijmans CM, van Loosdrecht MCM, Brdjanovic D. 2016. Prevalence of ‘Candidatus Accumulibacter phosphatis’ type II under phosphate limiting conditions. AMB Express 6.

63. Wexler M, Richardson DJ, Bond PL. 2009. Radiolabelled proteomics to determine differential functioning of Accumulibacter during the anaerobic and aerobic phases of a bioreactor operating for enhanced biological phosphorus removal. Environ Microbiol 11:3029–3044.

64. Barr JJ, Dutilh BE, Skennerton CT, Fukushima T, Hastie ML, Gorman JJ, Tyson GW, Bond PL. 2016. Metagenomic and metaproteomic analyses of Accumulibacter phosphatis-enriched floccular and granular biofilm. Environ Microbiol 18:273–87.

65. Kim J, Chang JH, Kim K-J. 2014. Crystal structure and biochemical properties of the (S)-3- hydroxybutyryl-CoA dehydrogenase PaaH1 from Ralstonia eutropha. Biochem Biophys Res Commun 448:163–168.

66. Barycki JJ, O LK, Strauss AW, Banaszak LJ, Author C, Banaszak Dietrich Professor LJ. 2000. Sequestration of the Active Site by Interdomain Shifting: Crystallographic and Spectroscopic Evidence for Distinct Conformations of L-3-Hydroxyacyl-CoA

Dehydrogenase Running Title: Human L-3-Hydroxyacyl-CoA Dehydrogenase. JBC Pap Press Publ.

67. Haywood GW, Anderson AJ, Chu L, Dawes EA. 1988. The role of NADH- and NADPH-linked acetoacetyl-CoA reductases in the poly-3-hydroxybutyrate synthesizing organism Alcaligenes eutrophus. FEMS Microbiol Lett 52:264–259.

68. Ling C, Qiao G-Q, Shuai B-W, Olavarria K, Yin J, Xiang R-J, Song K-N, Shen Y-H, Guo Y, Chen G-Q. 2018. Engineering NADH/NAD+ ratio in Halomonas bluephagenesis for enhanced production of polyhydroxyalkanoates (PHA). Metab Eng 49:275–286.

69. Filipe CDM, Daigger GT, Grady CPL. 2001. A metabolic model for acetate uptake under anaerobic conditions by glycogen accumulating organisms: Stoichiometry, kinetics, and the effect of pH. Biotechnol Bioeng 76:17–31.

70. García Martín H, Ivanova N, Kunin V, Warnecke F, Barry KW, McHardy AC, Yeates C, He S, Salamov A a, Szeto E, Dalin E, Putnam NH, Shapiro HJ, Pangilinan JL, Rigoutsos I, Kyrpides NC, Blackall LL, McMahon KD, Hugenholtz P. 2006. Metagenomic analysis of two enhanced biological phosphorus removal (EBPR) sludge communities. Nat Biotechnol 24:1263–1269.

71. Van Winden W, Verheijen P, Heijnen S. 2001. Possible pitfalls of flux calculations based on13C-labeling. Metab Eng 3:151–162.

72. Gottschalk G. 1986. Bacterial Metabolism. Springer New York, New York, NY.

73. Burow LC, Mabbett AN, Blackall LL. 2008. Anaerobic glyoxylate cycle activity during simultaneous utilization of glycogen and acetate in uncultured Accumulibacter enriched in enhanced biological phosphorus removal communities. ISME J 2:1040–51.

74. Skennerton CT, Barr JJ, Slater FR, Bond PL, Tyson GW. 2015. Expanding our view of genomic diversity in Candidatus Accumulibacter clades. Environ Microbiol 17:1574–1585.

75. Wilmes P, Andersson AF, Lefsrud MG, Wexler M, Shah M, Zhang B, Hettich RL, Bond PL, VerBerkmoes NC, Banfield JF. 2008. Community proteogenomics highlights microbial strain-variant protein expression within activated sludge performing enhanced biological phosphorus removal. ISME J 2:853–864.

76. He S, McMahon KD. 2011. “Candidatus Accumulibacter” gene expression in response to dynamic EBPR conditions. ISME J 5:329–340.

77. Erdal UG, Erdal ZK, Daigger GT, Randall CW. 2008. Is it PAO-GAO competition or metabolic shift in EBPR system? Evidence from an experimental study. Water Sci Technol 58:1329–34.

78. Lawson CE, Strachan BJ, Hanson NW, Hahn AS, Hall ER, Rabinowitz B, Mavinic DS, Ramey WD, Hallam SJ. 2015. Rare taxa have potential to make metabolic contributions in enhanced biological phosphorus removal ecosystems. Environ Microbiol 17:4979–4993.

79. Lemos PC, Serafim LS, Santos MM, Reis M a M, Santos H. 2003. Metabolic Pathway for Propionate Utilization by Phosphorus-Accumulating Organisms in Activated Sludge: 13C Labeling and In Vivo Nuclear Magnetic Resonance. Appl Environ Microbiol 69:241–251.

80. Buckel W, Thauer RK. 2013. Energy conservation via electron bifurcating ferredoxin reduction and proton/Na+ translocating ferredoxin oxidation. Biochim Biophys Acta - Bioenerg 1827:94–113.